GEOLOGICAL SURVEY OF CANADA

OPEN FILE 3779

MULTI-CHANNEL SEISMIC REFLECTION SURVEY OVER THE NORTHERN QUEEN CHARLOTTE FAULT

M. Scheidhauer, A.M. Trehu,
K.M.M. Rohr

1999

Natural Resources Canada | Ressources naturelles Canada

Canada

Multi-channel Seismic Reflection Survey over the northern Queen Charlotte Fault
Geological Survey of Canada Open File No. 99-xxx

M.Scheidhauer, Oregon State University, A.M.Trehu, Oregon State University, and K.M.M.Rohr, Geological Survey of Canada

INTRODUCTION

Multi-channel seismic reflection data were collected by the R/V *Ewing* over the Queen Charlotte Fault (QCF) during the ACCRETE project (Fig. 1) (Diebold, 1994). Line 1250 was collected while steaming from the Pacific plate towards the interior of the North American plate. Lines 1262-1265 were collected at the end of the planned ACCRETE work; these lines were planned to look in more detail at the QCF and associated structures.

The Queen Charlotte Fault is a transform plate boundary between the Pacific and North American plates. At the latitude of study the relative motion is slightly transpressive. A geomorphic terrace of faulted and folded sediments lies west of the QCF. The dynamics and deeper composition of this feature have been enigmatic. Refraction and gravity studies across the terrace showed velocities and densities lower than those of oceanic and continental crust (Dehler and Clowes, 1988). Shooting across the relatively narrow terrace resulted in a small number of rays that soled in this structure. One of the goals of lines 1263 - 1265 was to test the feasibility of collecting data along the terrace; the question being whether side echos would predominate in the records. This was not the case; very good records were in fact obtained along most of the profiles.

A joint study by the US Geological Survey and the Geological Survey of Canada collected multi-channel data in the same area in 1977 using the *SP Lee.* Data from this survey were stacked and an interpretation of one line across Dixon Entrance was published (Snavely et al., 1981; Rohr et al., 1992).

In this Open File we present the processing sequence, and stacked, migrated and interpreted sections for the ACCRETE dataset as well as interpreted sections from the data collected in 1977 (Plates 17,18,20a and 20b).

ACQUISITION

The airgun array consisted of 20 guns for a total volume ot 8400 in^3 (138 L) and was towed at a depth of 7 m. Shots were fired at average times of 20 s with a deliberately randomized variation of +/- 500 ms. This resulted in shot spacing varying from 45-60 m apart. The streamer had 224 channels with a group spacing of 12.5 m for a total length of 2800 m. The first receiver (channel 224) was 175 m from the centre of the airgun array.

The field data were recorded in SEG-Y format at a sampling rate of 4 milliseconds. An anti-aliasing high-cut filter of 125 Hz was applied in the field prior to digitisation. The total trace length was 16.5 seconds.

Using GPS navigation the shotpoint data were sorted into common-midpoint (cmp) format with a bin size of 12.5 m. This resulted in cmp's with an average fold of 60.

Table 1. Shot point-numbers, corresponding cmp's and the maximum folds of the lines processed.

	Shot point number	cmp's	cmp spacing	max. fold
Line 1250	101 to 1662	275 to 7000	12.5	68
Line 1262	22924 to 24489	4621 to 11626	12.5	68
Line 1263	24534 to 26230	275 to 7630	12.5	66
Line 1264	26260 to 27401	275 to 5191	12.5	62
Line 1265	27456 to 27920	275 to 2280	12.5	56

PRE-STACK PROCESSING

Processing followed the basic steps of computing cmp geometry, editing shotpoints, performing a cmp sort, analysing velocities, stacking and migrating. Lines 1250 and 1262, 1264 and 1265 were processed at Oregon State University (OSU) (Scheidhauer, 1997) using Sioseis software and line 1263 was processed at the Geological Survey of Canada (GSC) using Insight software. A flowchart of data processing steps (Table 2) summarizes the processing sequence applied to lines 1250, 1262, 1264 and 1265.

Table 2. Processing flowchart showing processing sequence used at OSU for Lines 1250, 1262, 1264 and 1265.

field tapes	***cmp-domain processing***	***post-stack processing***
1. preprocessing	**4. cmp sort**	**9. premigration processes**
	⇓	⇓
	5. velocity analysis	- bandpass filter (10-60 Hz)
	⇓	⇓
-cmp geometry in trace headers	**6. time-variant band-pass filter**	- mute water-bottom multiple
⇓	⇓	⇓
2. trace edit of shotpoints	**7. NMO-correction**	$-t^2$-gain
⇓	⇓	
	8. stack	**10. finite-difference migration**
	⇓	

Table 3. Processing flowchart showing processing sequence used at GSC for line 1263.

field tapes	***cmp-domain processing***	***post-stack processing***
1. preprocessing	**4. cmp sort**	**9. premigration processes**
	⇓	⇓
	5. velocity analysis	- bandpass filter (10-60 Hz)
	⇓	⇓
-cmp geometry in trace headers	**6. time-variant band-pass filter**	- mute water-bottom multiple
⇓	⇓	⇓
2. trace edit of shotpoints	**7. NMO-correction**	
⇓	⇓	

energy balance spherical divergence correction filter 15-70 Hz	**8. stack** ⇓	**10. finite-difference migration**

Common Shot Gathers

The common shot gather of shot 23000, Line 1262 (Fig. 2a) is typical of many of the shotpoints in that it shows a decay of amplitudes with time, bad traces and tow noise on the far offsets. Multiples were a significant source of noise and in water deeper than approximately 1 s, were strong enough to overwhelm whatever primary reflection energy might have been there.

The steep continental slope and ridges that define the western edge of the terrace were sources for side or back scattering because of their dip and rough surfaces. Figure 4 shows back scattered energy in shot-gather 23500 which was located along the slope; stacking significantly reduced this noise.

Traces 5, 149, 150, 195, 214 and 219 were either dead, noisy or reversed and were edited out i.e. not included in further work.

No low-pass filter was used on the data during acquisition so significant amounts of low-frequency tow noise were recorded (Fig. 2 and 3). A band-pass filter eliminated the lowest frequencies of tow-noise but some of it was in the same frequencies as the reflections (Figs. 2-4).

To determine the frequency content of the shot gathers, a fast Fourier transform of six traces from shot 23000 was performed (Fig. 2b). Figure 2c demonstrates the effect of a 39-point time domain 10-100 Hz bandpass filter on shot gather 23000. Compared with Figure 2a the signal to noise (S/N) ratio is improved.

A time-varying bandpass filter was applied to shot gathers in hopes of reducing the multiples. The convolutional zero-phase filter length was 39 points (156 ms) and the passband was 10-100 Hz before the multiple, and 10-40 Hz after the multiple for the shelf area and 10-50 Hz after the multiple on the rise and abyssal plain data. The lower frequency band of 10-40/50 Hz was used to eliminate the higher frequency portion of the multiples; deeper reflections tend to have lower frequency content.

Figure 3b shows the amplitude spectra of all traces from shotpoint 25602, Line 1263 (Fig. 3a). A Butterworth band pass of 15-75 Hz was applied to these data (Fig. 3c). On 1263 a trace balance was performed to ensure that the energy of each trace was identical using data between 0 and 8 s to estimate energy. To counteract spherical spreading, a gain was applied which is based on the distance traveled by each ray; it varied with time and offset. Distance was calculated from preliminary velocity functions obtained by semblance analyses of shotpoints at six different sections of the line.

During shooting of 1263 the far offset sections of the streamer were floating close to the sea surface resulting in significant noise on the data (Fig. 5a). Slowing the ship down resulted in the streamer settling to reasonable depths and quieter data for lines 1264 and 1265. Band pass filtering was unable to remove all of the noise so surgical muting was applied to far offset data on the first section of line 1263 (Fig. 5b). The low cut of the prestack bandpass filter was raised to 17 Hz for cmps 5000-5195 of line 1264 and for cmps 275-560 and 901-1160 of line 1265. On Line 1250 a low cut of 20 Hz instead of 10 Hz was chosen between cmps 550-750, due to the increased low frequency noise in this area.

Velocity Analysis and Stacking

Two different methods were used to conduct velocity analyses: the constant velocity and the velocity spectrum method. Semblance contour plots were calculated for every 100th cmp (1.25 km) of each profile. Figure 6B shows a semblance contour plot for cmp 11100 of line 1262 (Fig. 6A), located on the Queen Charlotte Trough over oceanic crust. This is a good example of how semblance contour peaks are located at continuously greater stacking velocities as two-way travel-time (twtt) increases. Starting at 3.5 seconds water depth, the black line follows the velocity function picked for this cmp. Semblance peaks of the water-bottom multiple (WBM) first appear at 7 s twtt and line up for consecutive depths along the water velocity of about 1500 m/s. Although stacking velocities for primary and multiple reflections differ by as much as 1500 m/s multiple energy still swamps the faint energy from genuine reflections.

Figure 7 shows a semblance contour plot of cmp 10500, where the S/N ratio is significantly reduced by diffracted energy due to topographic relief and dipping events. In this plot, strong semblance peaks are only visible above 3.7 seconds, and their appearance is more scattered than at comparable depths in Figure 6B.

To find the optimum velocity distribution for the whole profile, a set of velocity functions was determined at every 100th cmp-control point. Stacking cmp gathers at these control points gave a first insight of how well reflections have been imaged. Stacking of the whole profile or portions of it revealed the quality of the two-dimensional velocity field, which can be seen in the continuity of reflectors. To verify velocities at specific cmps, constant velocity panels were used to pick velocities and improve the stack.

Figures 8-12 display the two-dimensional stacking velocity distribution for each line. These stacking velocity distributions were used for normal moveout correction and stacking. Far offset data which were stretched beyond 500 ms were muted automatically during the normal moveout process. For line 1263 any stretch beyond 20% of the original wavelet length resulted in a mute being applied.

On Line 1263 the faulted sections of the stack received dip moveout processing and a second pass at calculating semblance and picking stacking velocities.

POST-STACK PROCESSESING

Post-stack processing was for the most part concerned with improvement of the display. A linear prediction deconvolution was applied to the shelf areas to reduce the water-bottom multiples, which appear at intervals of 0.34 seconds twtt. This time delay was input as the prediction distance. An autocorrelation of the design window was taken and an inverse filter was designed so that the autocorrelation of the same window after deconvolution resulted in a spike followed by zeros.

For plotting purposes, four adjacent traces (50 m) were mixed (added) in order to reduce the profile length and further attenuate random noise. All stacked sections were displayed by using an automatic gain control (AGC) with a time window of 1 second and the same constant scalar of 1.5E-07 to preserve amplitude relationships between traces. The horizontal scale is fixed at 130 mixed traces per inch and the vertical scale set to 0.5 inches per second resulting in a vertical exaggeration of 2.19.

Migration

Following stacking, migration was the last principal step of processing. The 45-degree-finite-difference algorithm was used to migrate the ACCRETE profiles. This method is capable of handling dips only up to angles of 45-degrees with sufficient accuracy. On the other hand, it handles lateral velocity variations reasonably well unless the changes are abrupt. This factor was considered to be important for the ACCRETE data, because the stacking velocity do vary laterally. In addition, steeply dipping reflectors are only significant at the westward boundary of the terrace and at the more steeply sloping portion of the terrace close to the shelf break. One important parameter of finite-difference migration is the depth-step size; a step size of 50 ms was chosen.

The finite-difference migrated profiles 1262, 1250, 1263, 1264 and 1265 are presented along with their structural interpretation (Plates 2-16). Energy below the first water-bottom multiple was muted before migration to prevent multiples from being migrated into the section. A t^2-gain correction was applied before migration except to line 1263 which received an AGC gain using a window 1 s long. Prior to migration the stacked section of 1263 was interpolated to a 6.25 m spacing to reduce the possibility of spatial aliasing. All data were filtered 10-60 Hz to further reduce any possibility of aliasing.

Some overmigration 'smiles' or smearing are still visible in the deeper parts of the terrace in lines 1262 and 1265. This could be due to bursts of high amplitude noise in the input section, which were migrated into smiles.

Overall, the finite-difference migration produced satisfactory results, except at the western edge of the terrace. Special treatment of strong dips before stacking is necessary there to properly image this region and to extract all possible structural information from the data.

REFERENCES

Dehler, S.A. and and Clowes, R.M., 1988, The Queen Charlotte Islands refraction project. Part I. The Queen Charlotte Fault Zone, C. J. Earth Sci., v. 25, p. 1857-1870.

Diebold, J., 1994, R/V EWING leg EW9412- "ACCRETE", 12 Sept - 22 Sept 1994 Prince Rupert B.C. - Prince Rupert B.C., Cruise Report, Lamont Doherty Earth Observatory.

Scheidhauer, 1997, Crustal Structure of the Queen Charlotte Transform Fault Zone from Multi-Channel Seismic Reflection and Gravity Data, M.Sc. Thesis Oegon State University

Snavely, P.D.Jr., Wagner, H.C., Tompkins, D.H., and Tiffin, D.L., 1981, Preliminary geologic interpretation of a seismic reflection profile across the Queen Charlotte Island fault system off Dixon Entrance, Canada, United States Geological Survey Open File report 81-299, 12p.

Rohr, K.M.M., Lowe, C. and Snavely, P.D.Jr., 1992, Seismic reflection, magnetic and gravity data across the Queen Charlotte Fault and Dixon Entrance, Geological Survey of Canada Open File Report 92-2615.

Yilmaz, O., 1988, Seismic data processing, Investigations in Geophysics, Society of Exploration Geophysics, Tulsa, OK, 526 p.

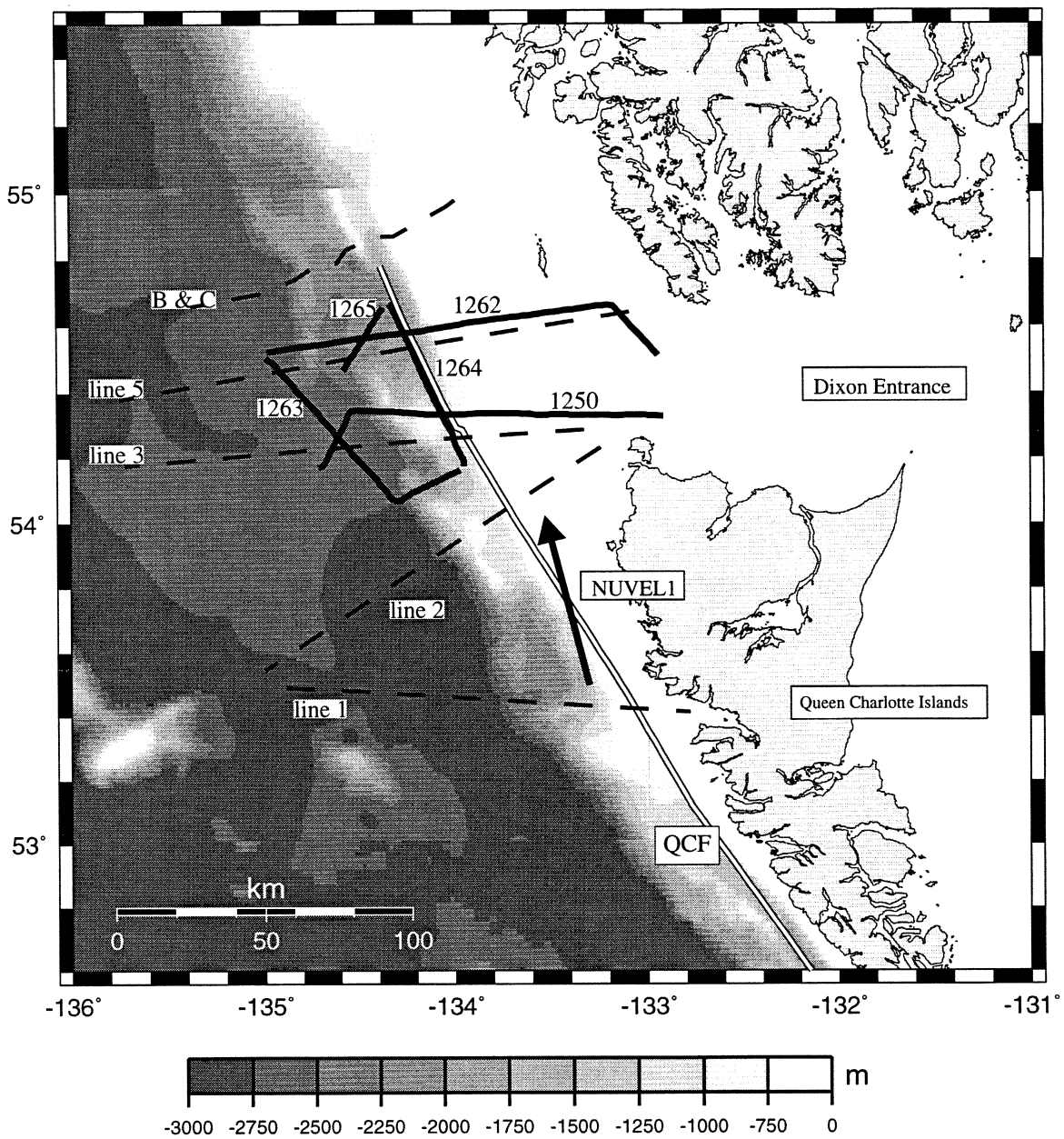

Figure 1: Bathymetry (in meters) of the study region, surrounding the Queen Charlotte Fault (white line); showing the well-resolved terrace segment with its triangular-shaped structure off Dixon Entrance and its more linear, block-like appearance west of the Queen Charlotte Islands.

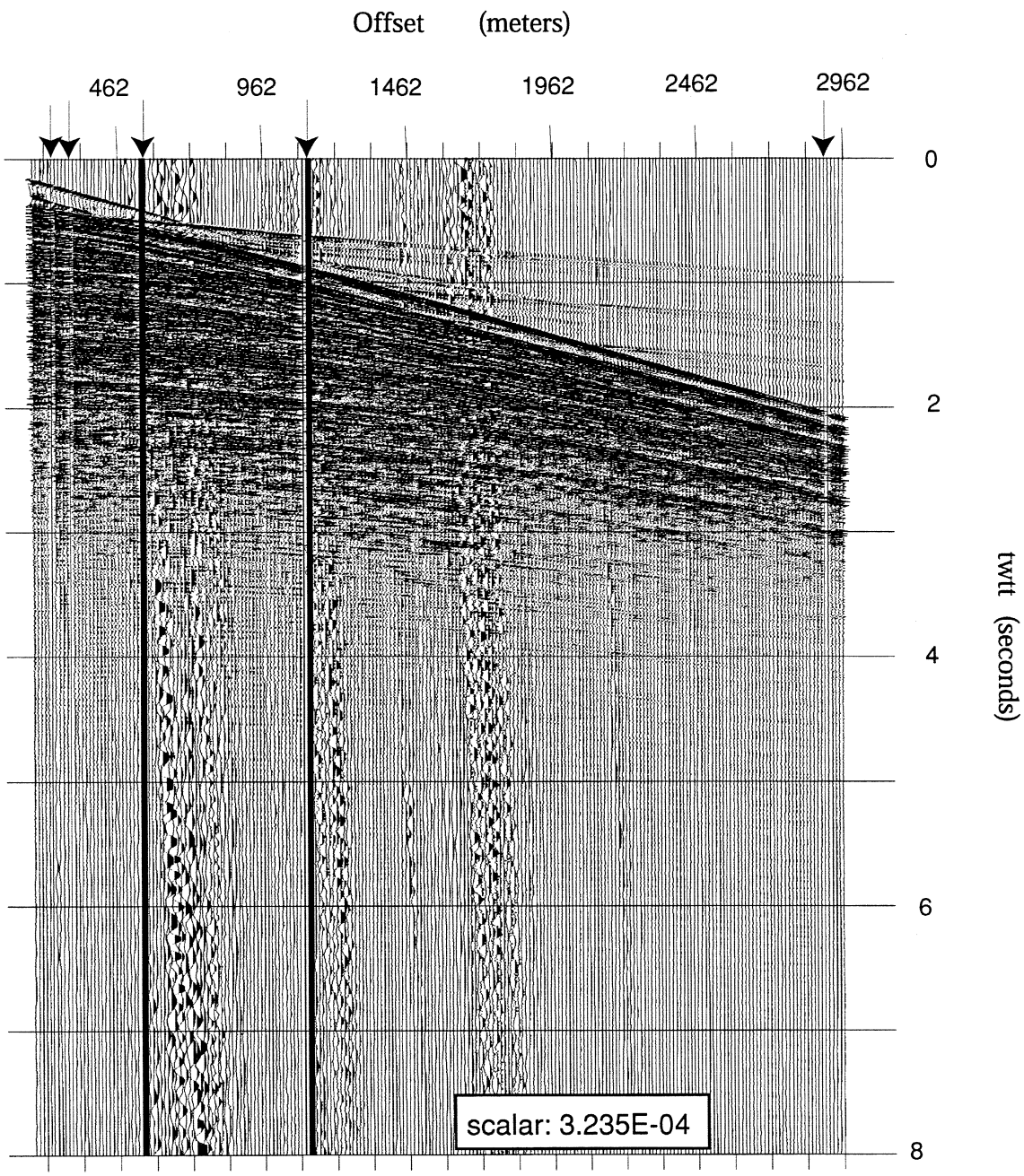

Figure 2A. Common shot gather of shot 23000 from line 1262 demonstrates the decay of signal amplitude with time and the presence of low frequency noise on some channels. Bad traces are marked by arrows.

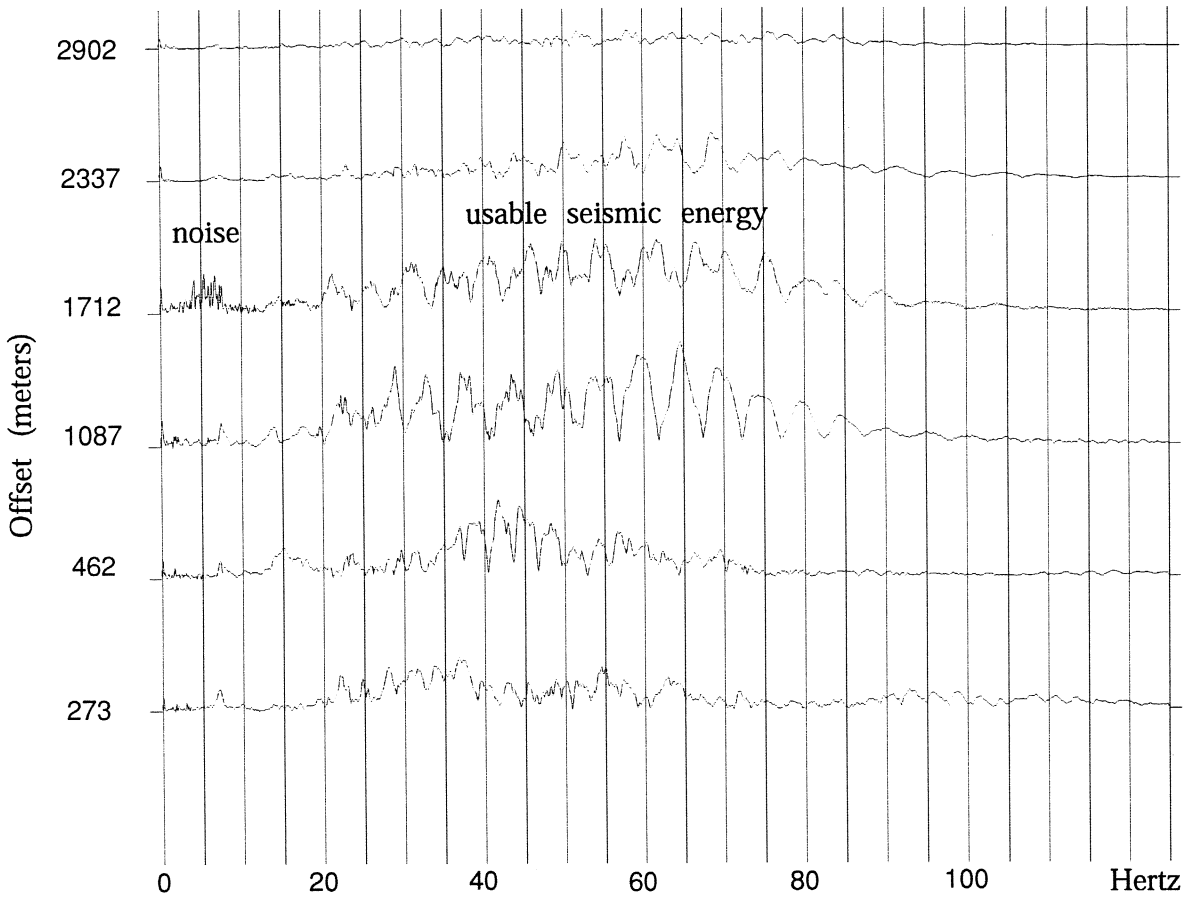

Figure 2B. Amplitude spectra of the fast Fourier transform of six traces for shot 23000 from line 1262, showing that the usable seismic energy lies in a range between 10-90 Hz. Low frequency random noise peaks about 6 Hz.

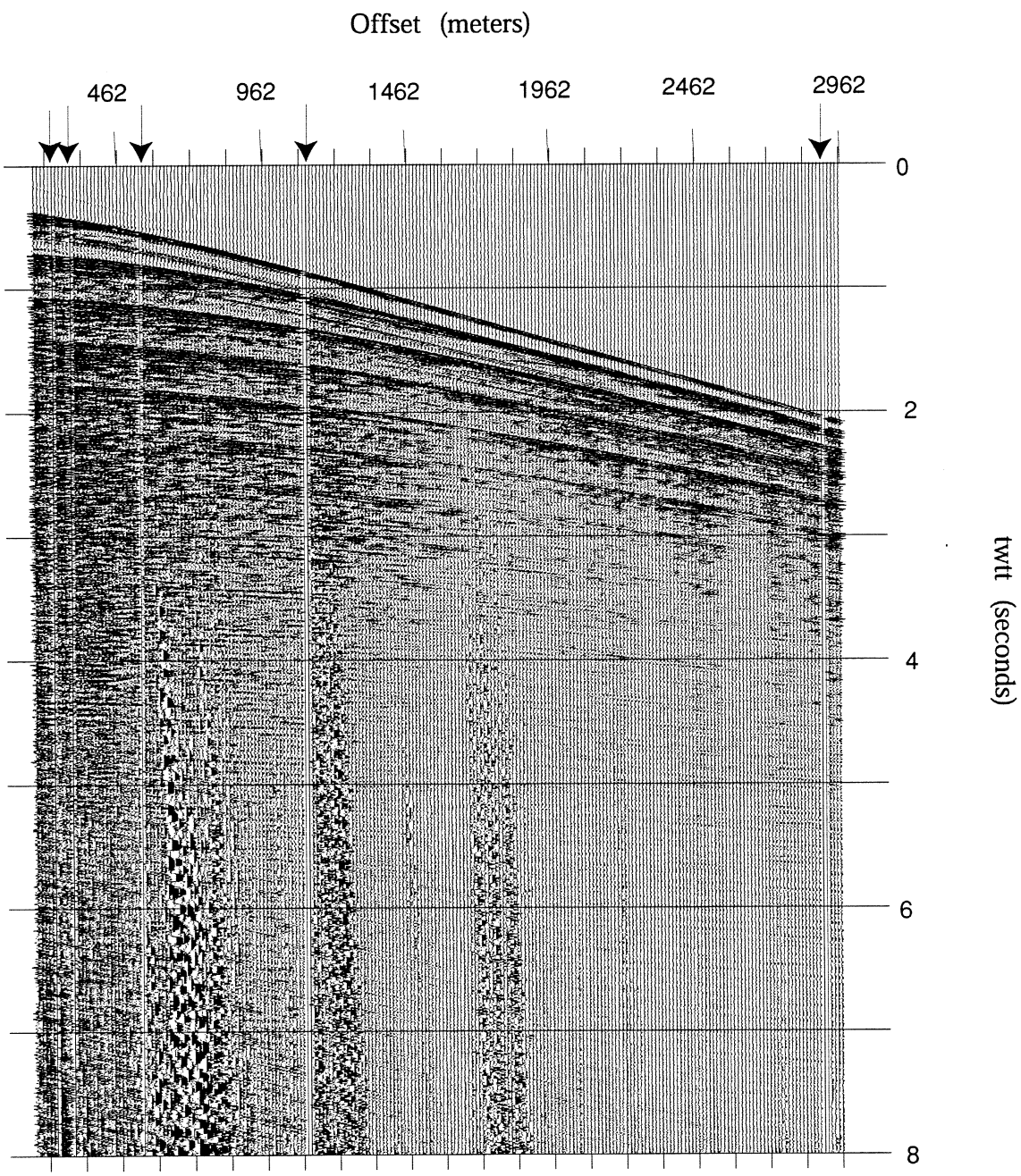

Figure 2C. Common shot gather of shot 23000 from line 1262 after application of a 39-point time domain 10-100 Hz bandpass filter. Compared with figure 2A, random noise is significantly attenuated.

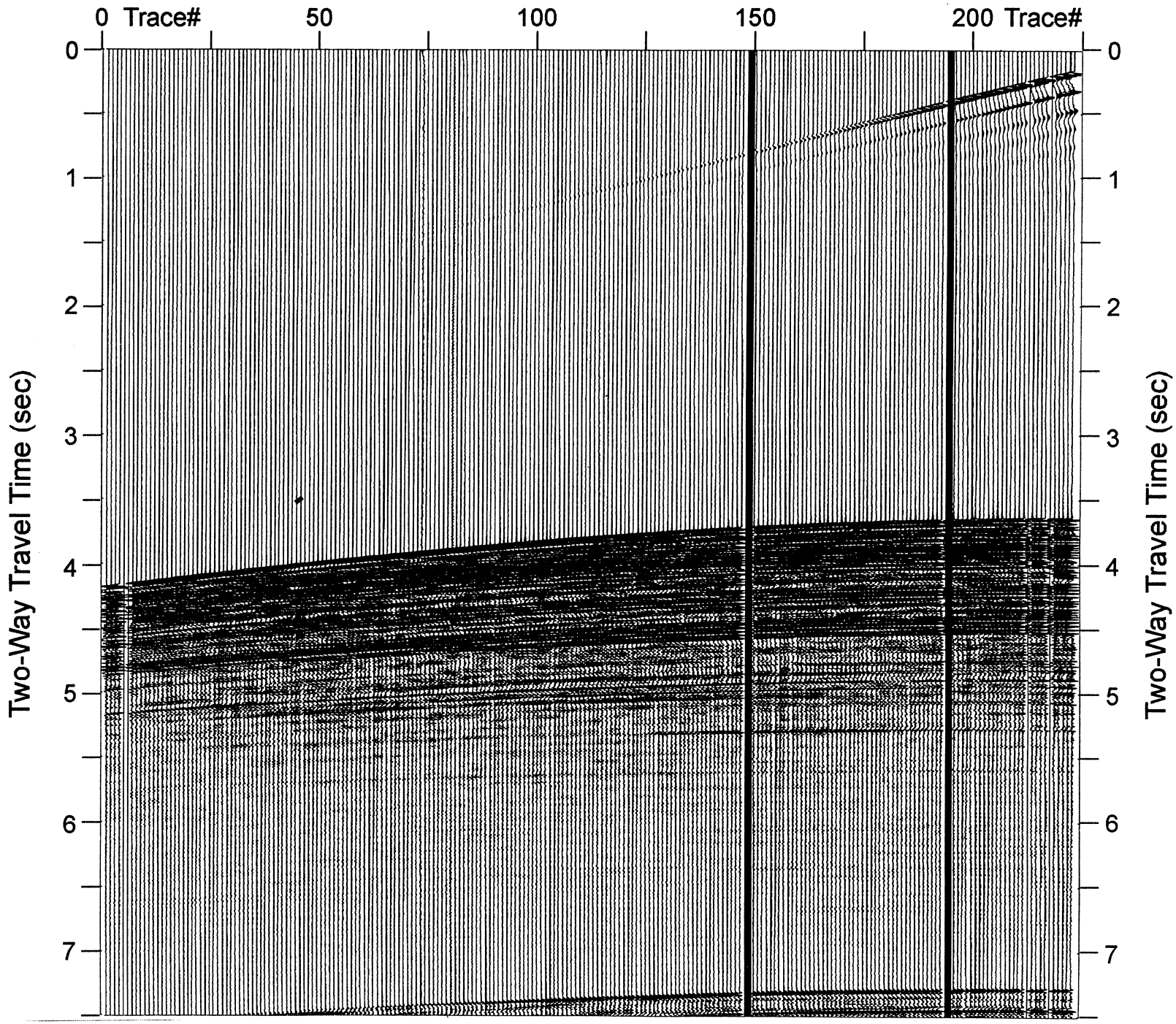

Figure 3a: Shotpoint 25602, line 1263.

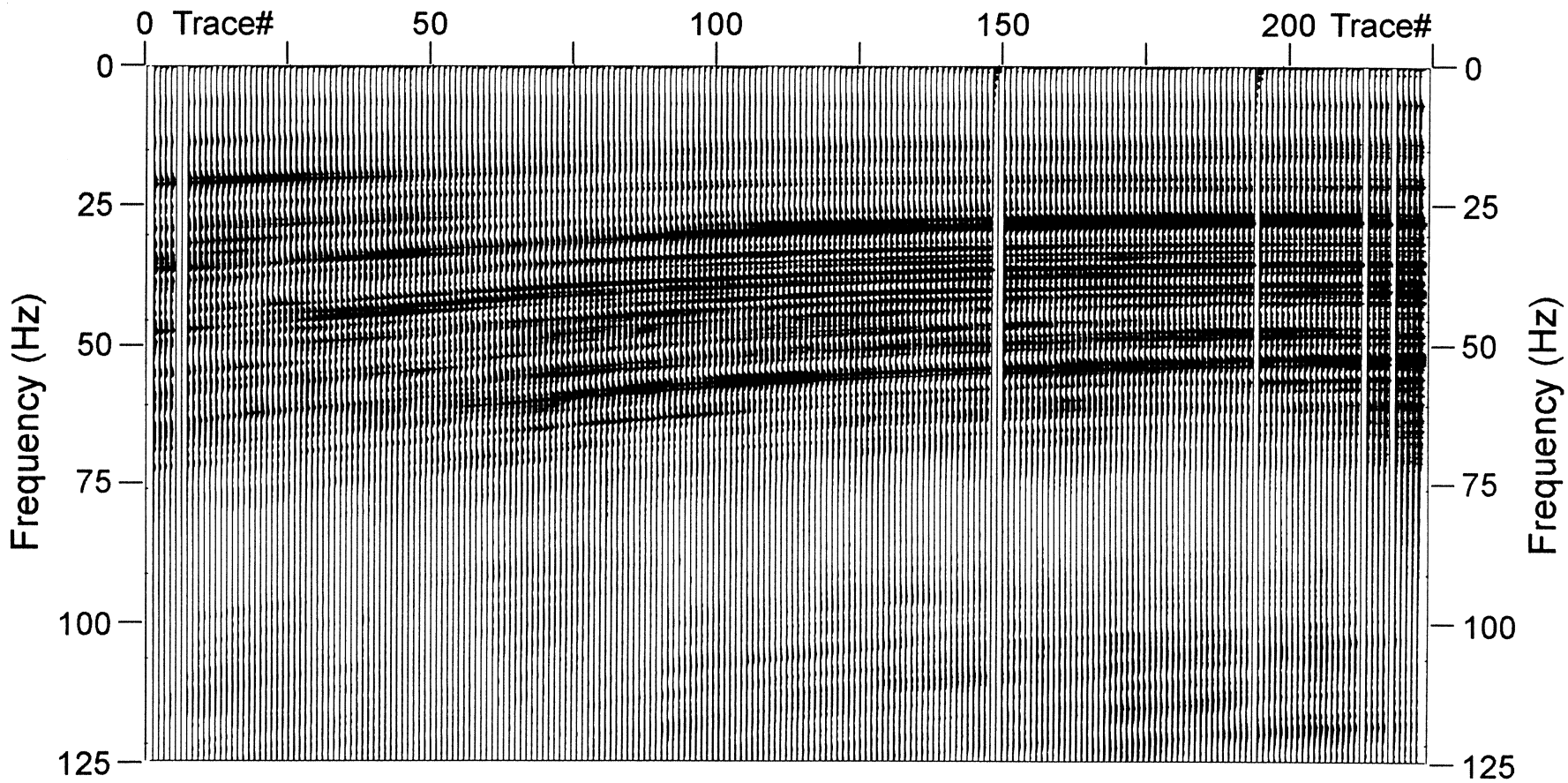

Figure 3b: Frequency content of shotpoint 25602, line 1263.

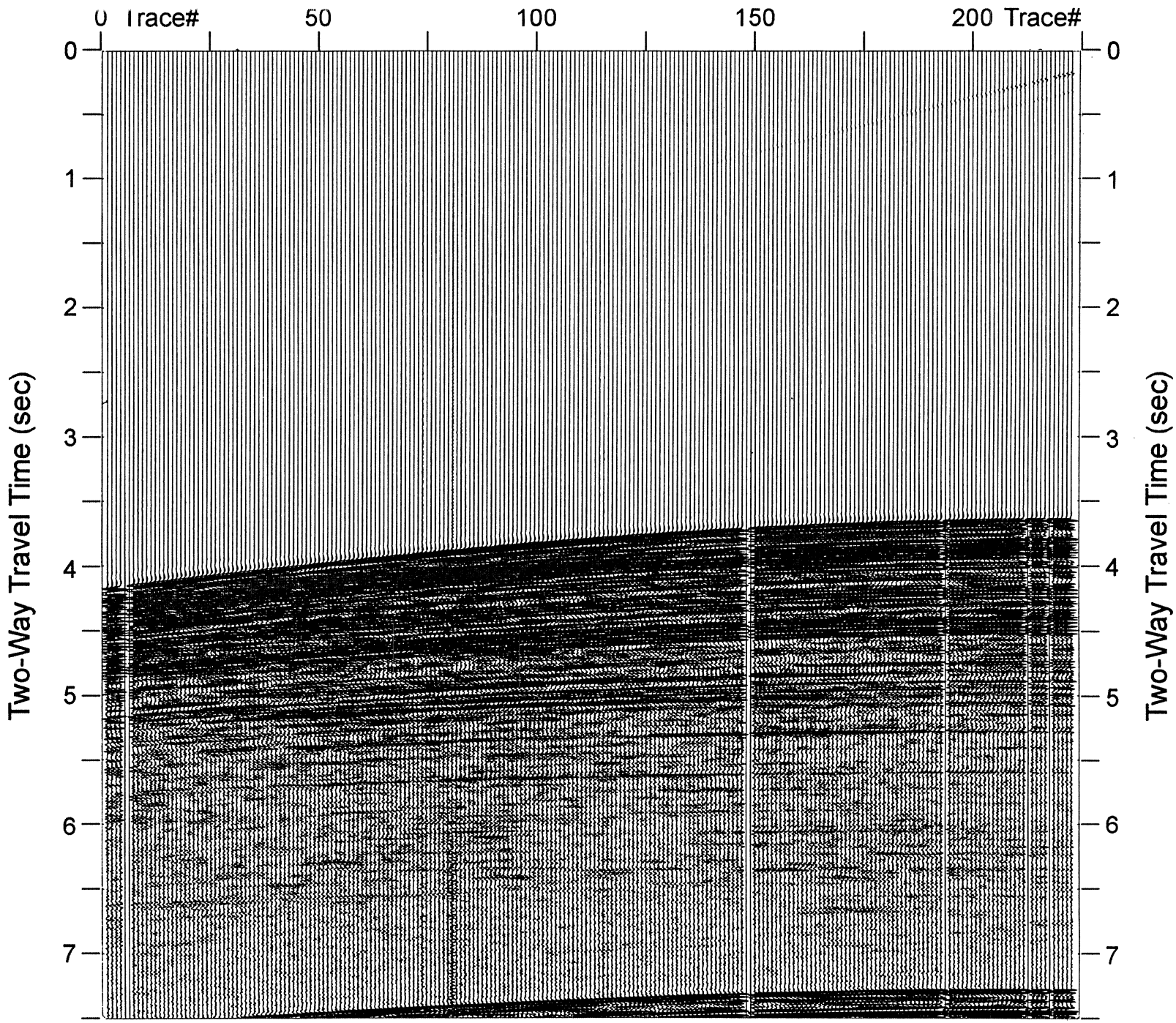

Figure 3c: Shotpoint 25602, line 1263, edited, filtered, gained and balanced.

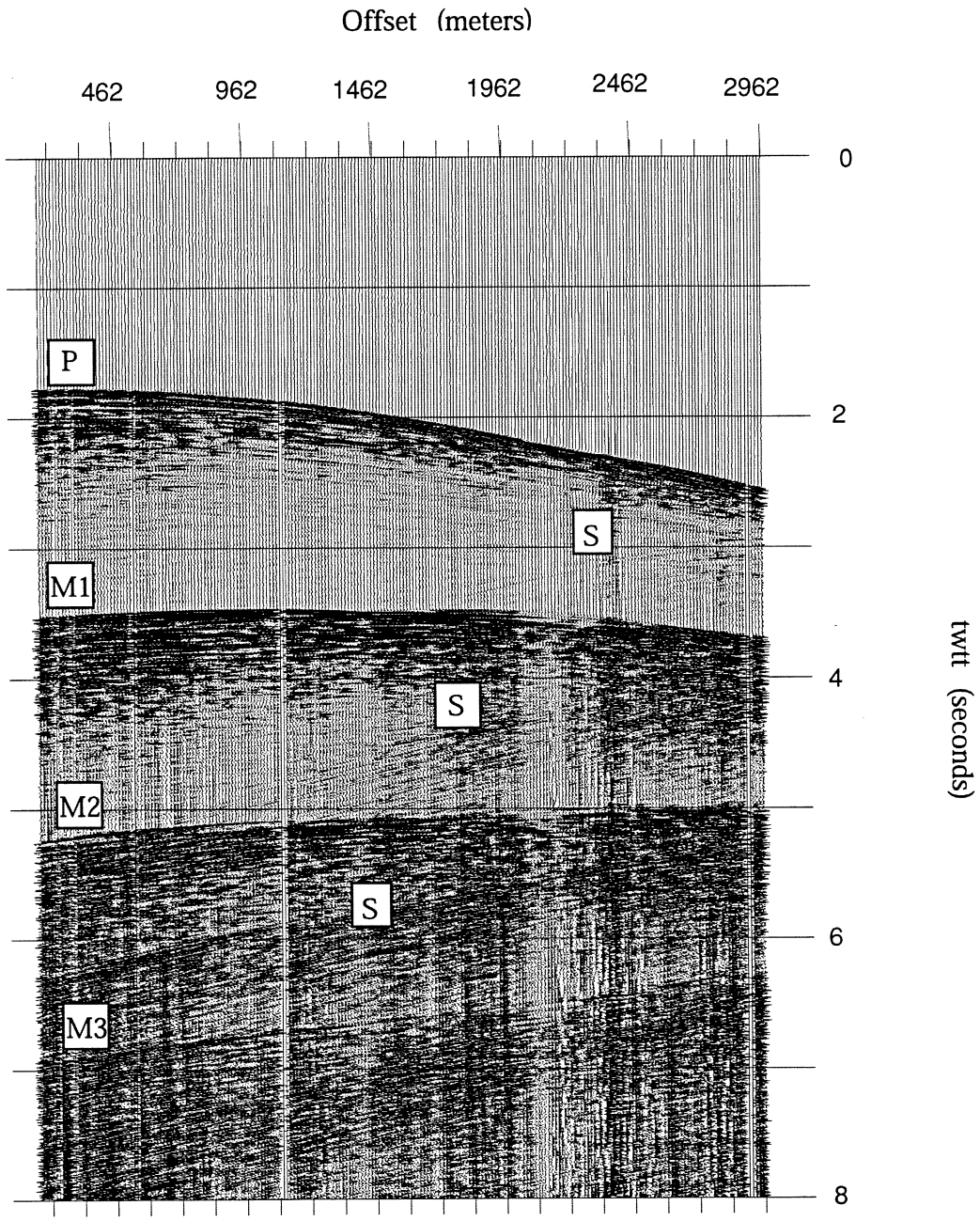

Figure 4. Common shot gather of shot 23500 on steeply sloping portion of the terrace, line 1262. Back-scattered energy is marked S. P, M1, M2, and M3 indicate the water-bottom reflection and its first and higher-order multiples.

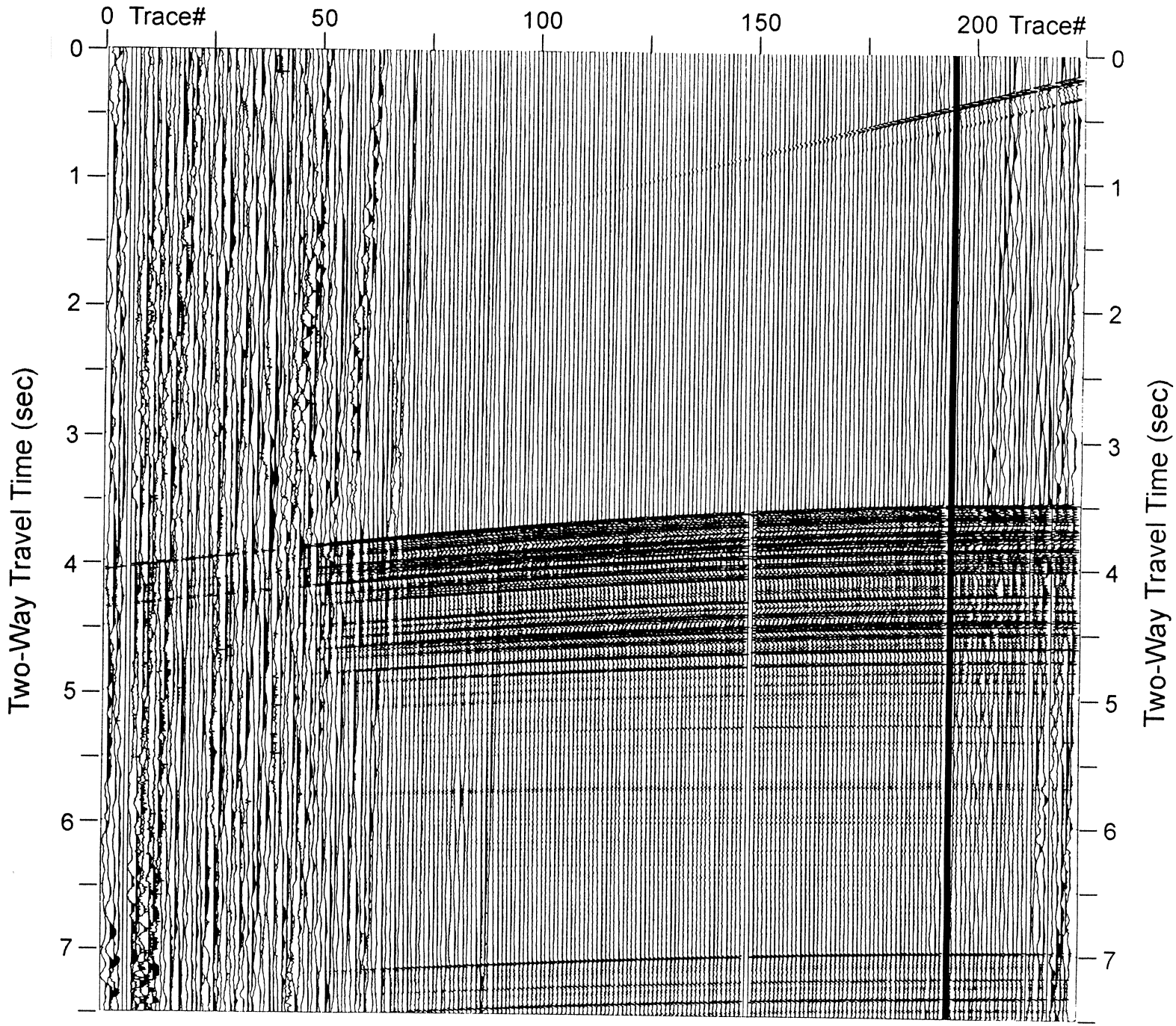

Figure 5a: Tow noise on shotpoint 24608, line1263

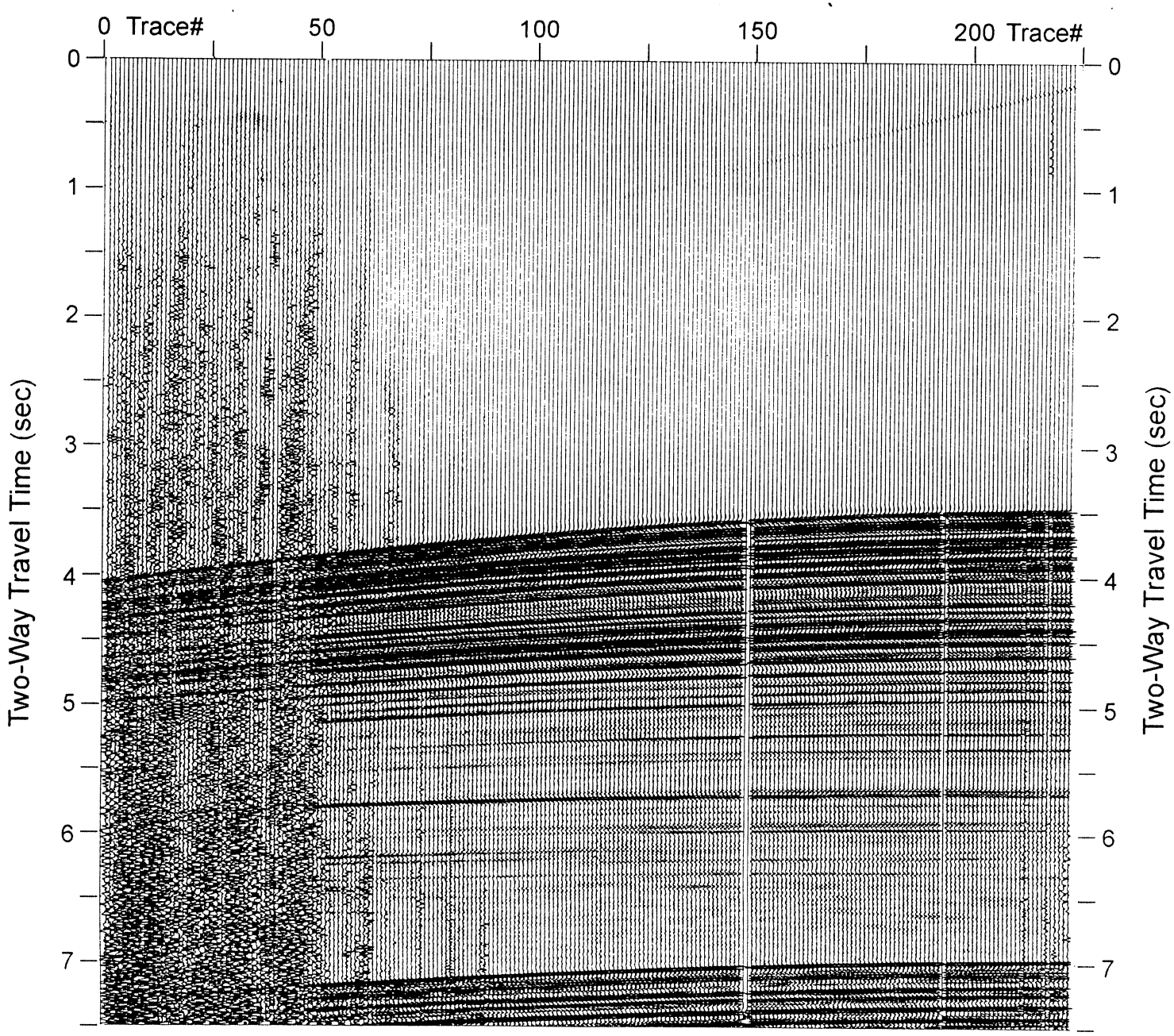

Figure 5b: Shotpoint 24608, line 1263, edited, filtered, gained and balanced.

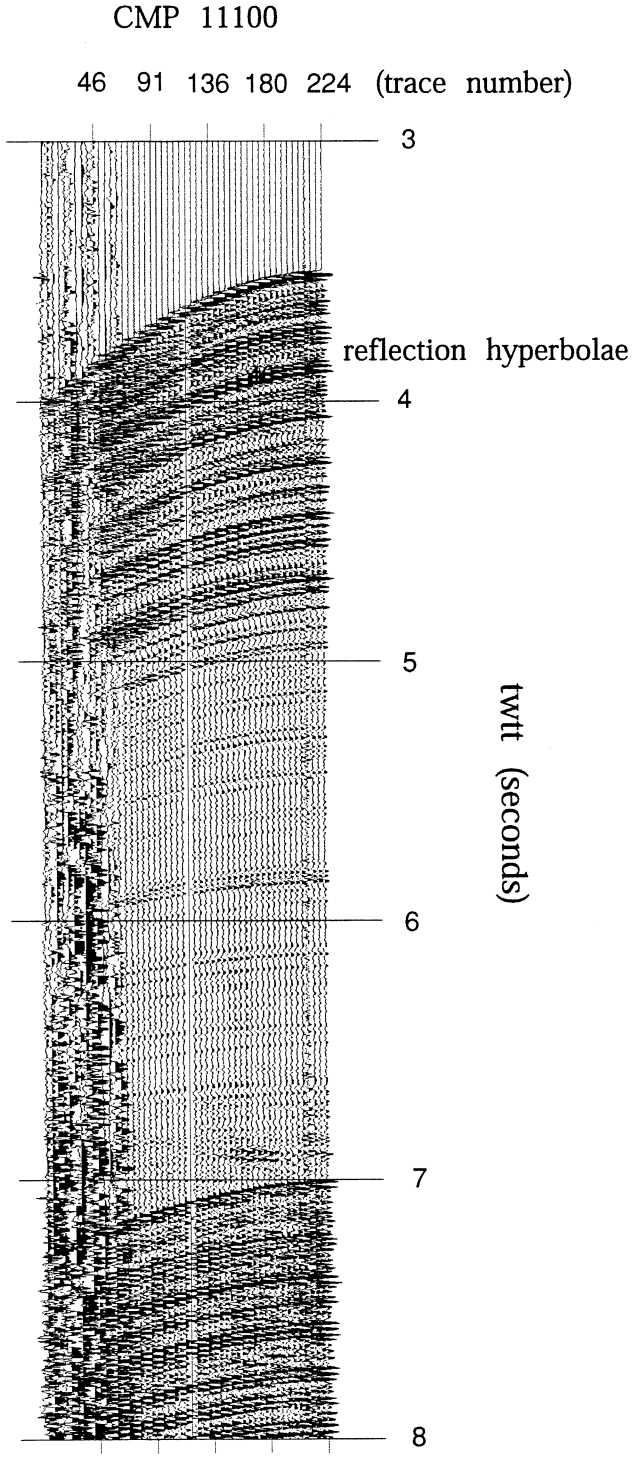

Figure 6A. Common mid-point gather of CMP 11100 in the trough segment of line 1262. A t^2-gain correction was applied as well as a time-domain bandpass filter with a passband of 10-125 Hz. Far-offset traces consist mainly of noise; reflections are distinguishable by their hyperbolic shape.

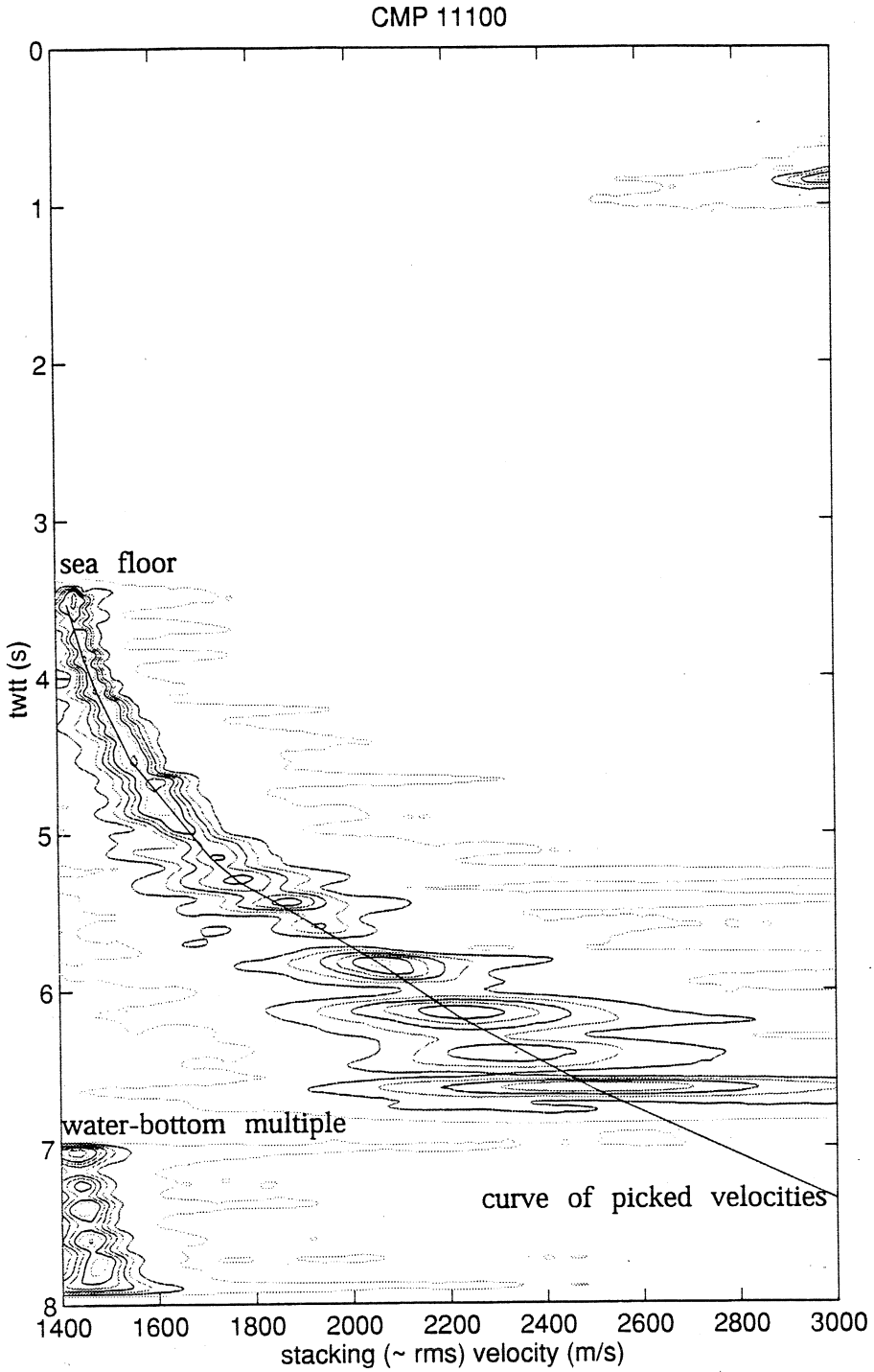

Figure 6B. Semblance contour plot (calculated with a 100 ms time gate and a velocity increment of 20 m/s) of CMP 11100 from line 1262 (Queen Charlotte Trough), showing how semblance contour peaks group around continuously greater velocities as twtt increases. Sea floor at 3.5 seconds twtt, with water bottom multiple at 7 seconds.

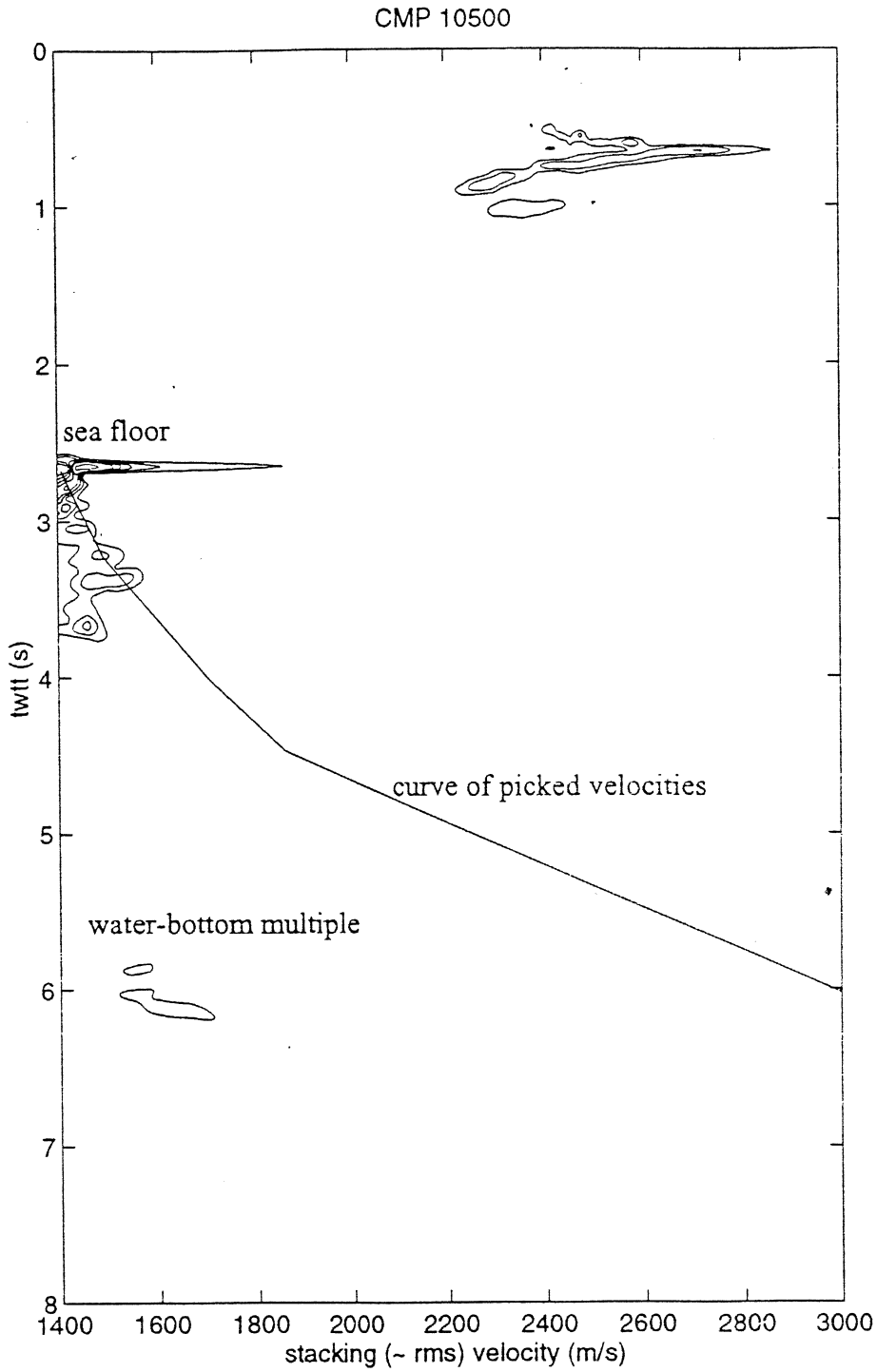

Figure 7: Semblance contour plot (calculated with a 100ms time gate and a velocity increment of 20m/s) of CMP 10500 of line 1262 located above rough surface on a ridge and dipping events; S/N ratio is significantly reduced by diffraction energy; semblance peaks are visible only above 3.7 seconds and are less focussed than those at comparable depths in figure 4.12.

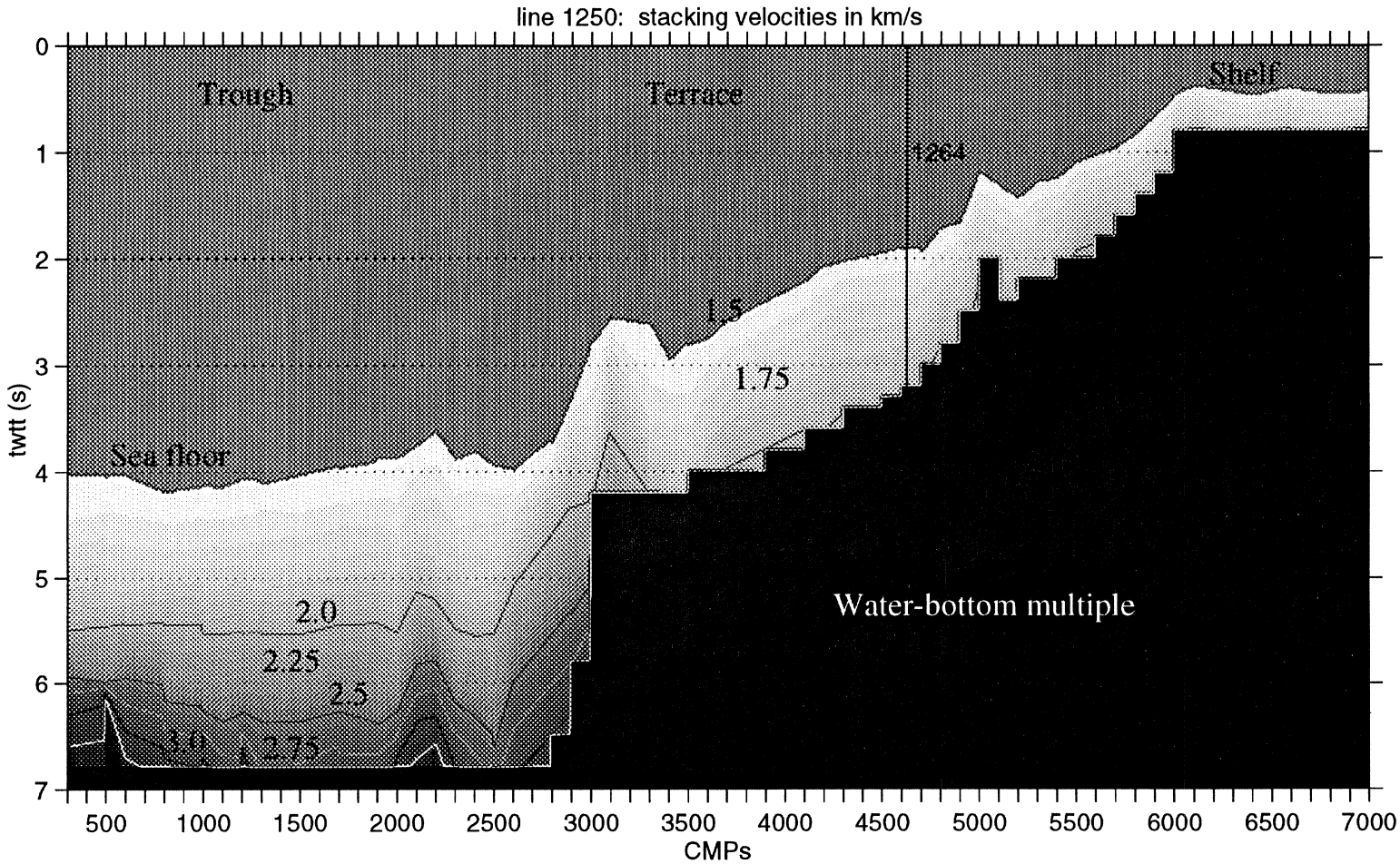

Figure 8: Two-dimensional stacking velocity distribution of line 1250 used for NMO correction; stacking velocity contours have intervals of 0.25 km/s. Velocity analyses were performed every 100th CMP. Grey area represents the water velocity of 1.5 km/s in shallow portions, and water-bottom multiples at depth are black.

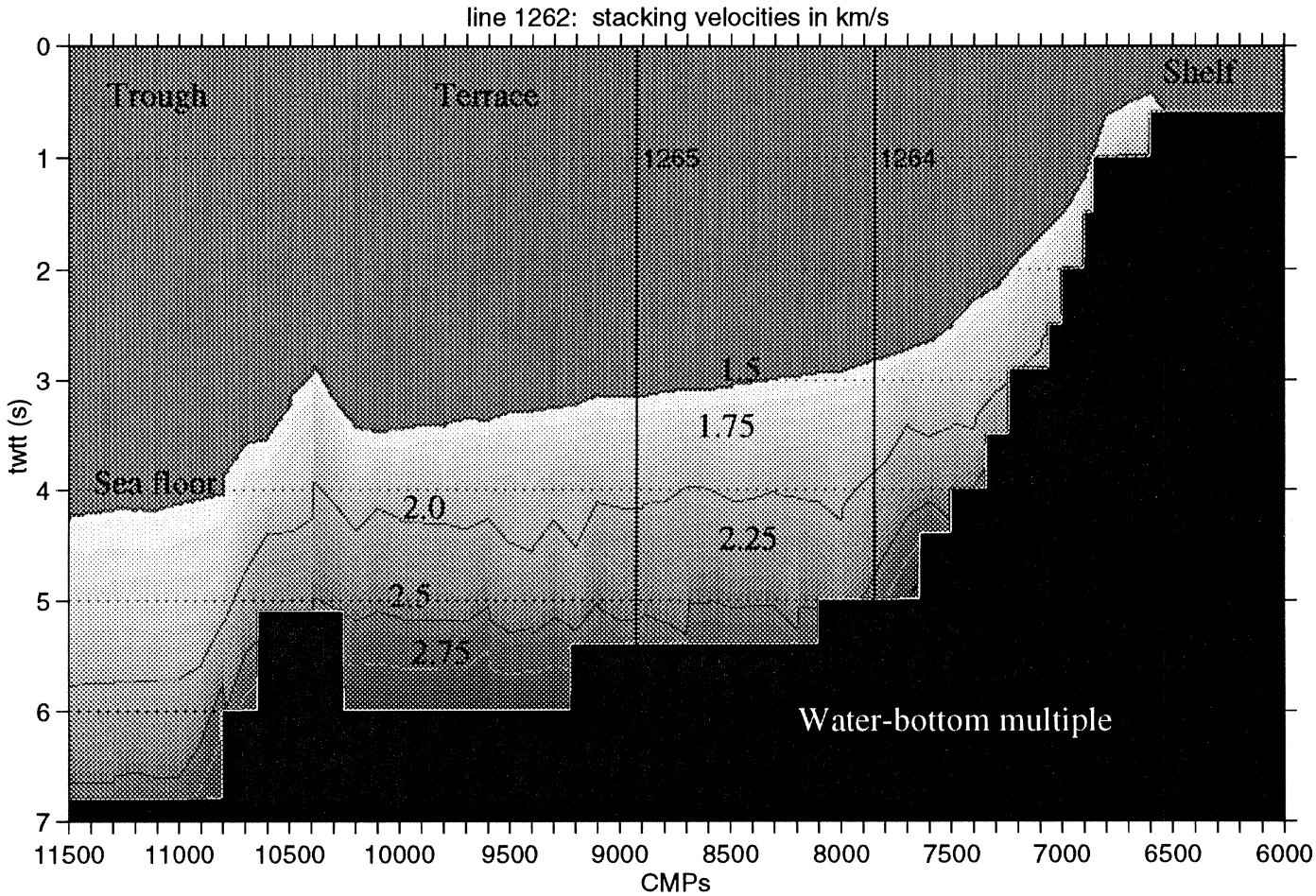

Figure 9: Two-dimensional stacking velocity distribution of line 1262 used for NMO correction; stacking velocity contours have intervals of 0.25 km/s. Velocity analyses were performed every 100th CMP. Grey area represents the water velocity of 1.5 km/s in shallow portions, and water-bottom multiples at depth are black.

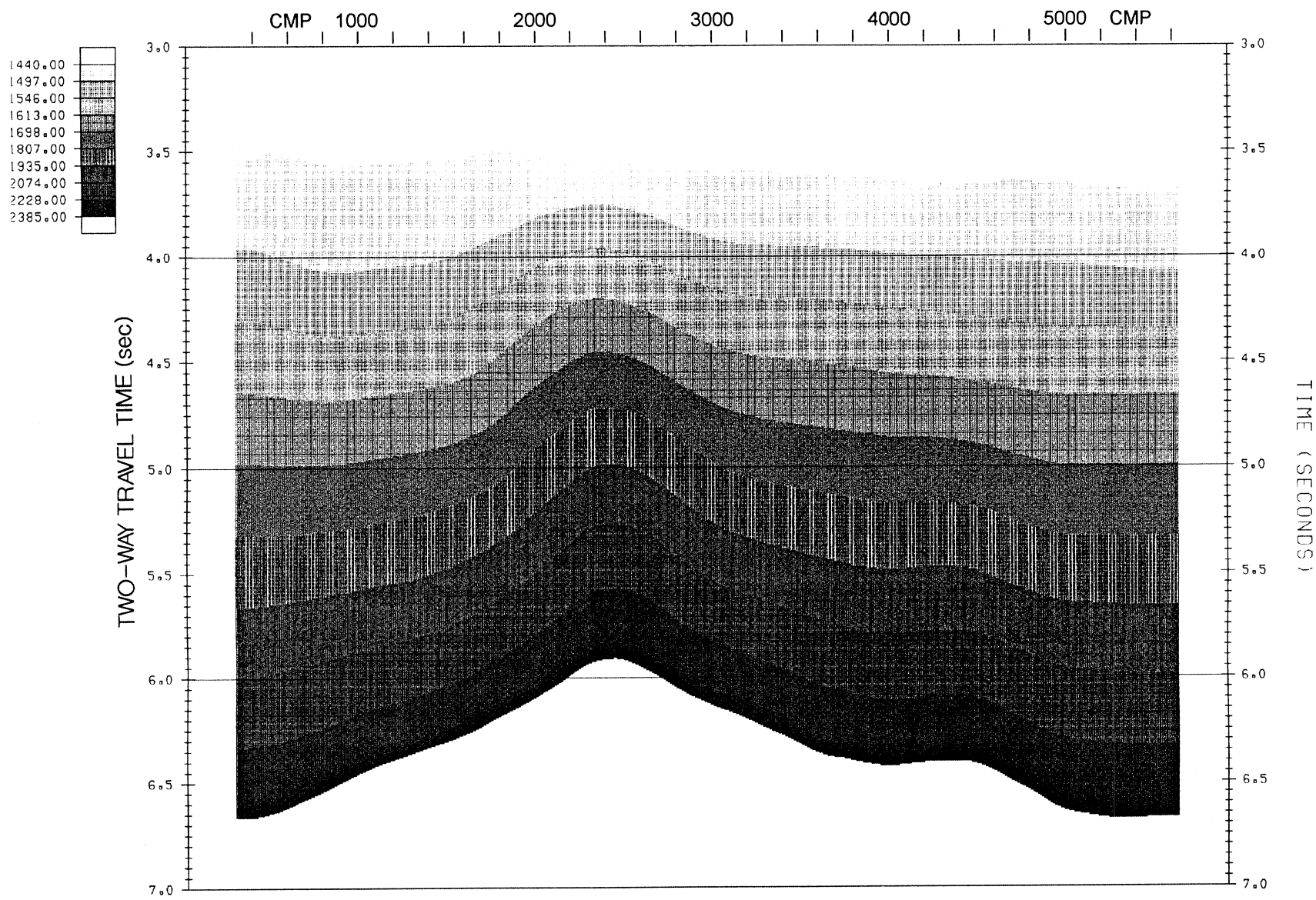

Figure 10: Two-dimensional stacking velocity distribution of line 1263 in the trough used for NMO correction. Velocity analysis were performed every 1.25km.

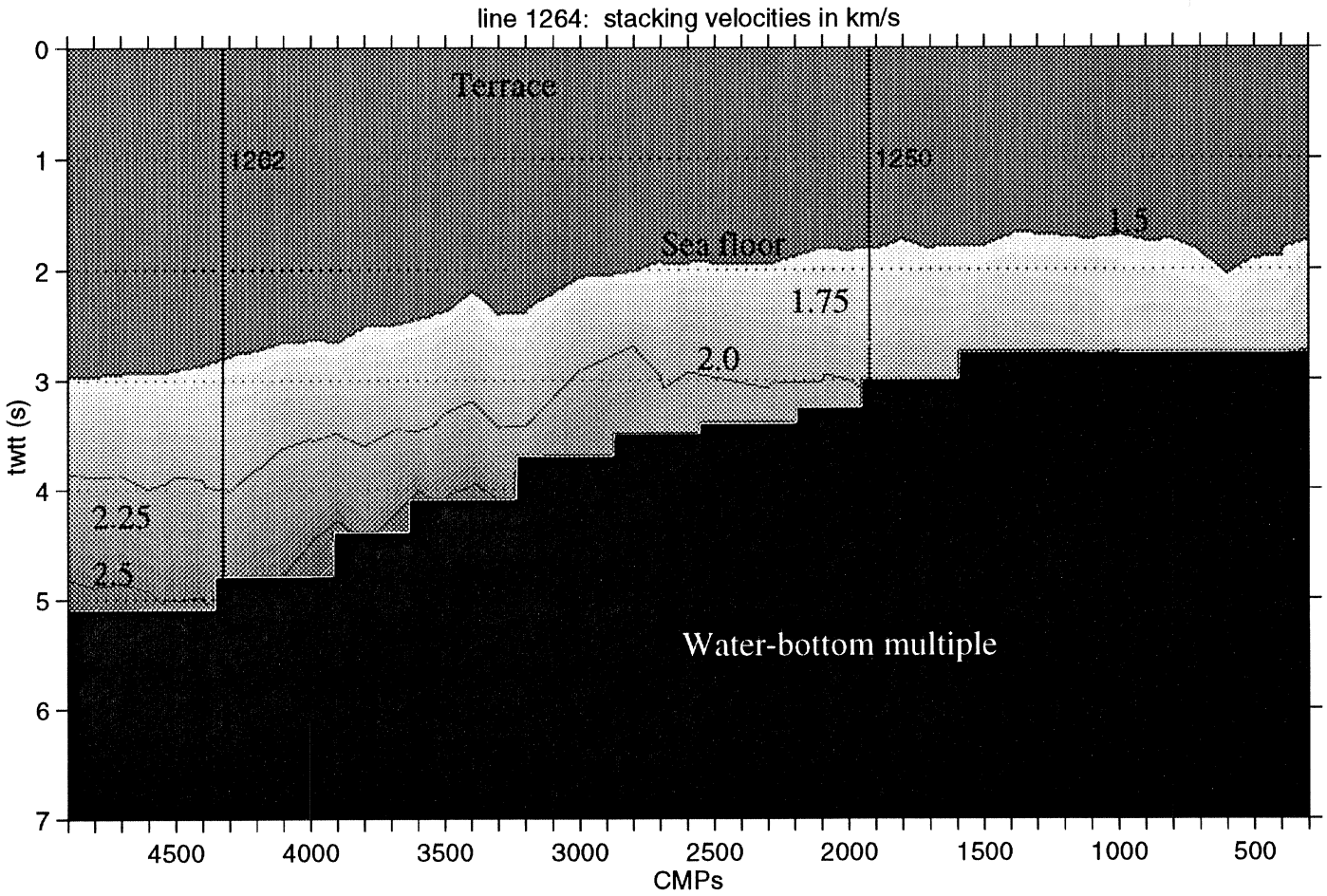

Figure 11: Two-dimensional stacking velocity distribution of line 1264 used for NMO correction; stacking velocity contours have intervals of 0.25 km/s. Velocity analyses were performed every 100th CMP. Grey area represents the water velocity of 1.5 km/s in shallow portions, and water-bottom multiples at depth are black.

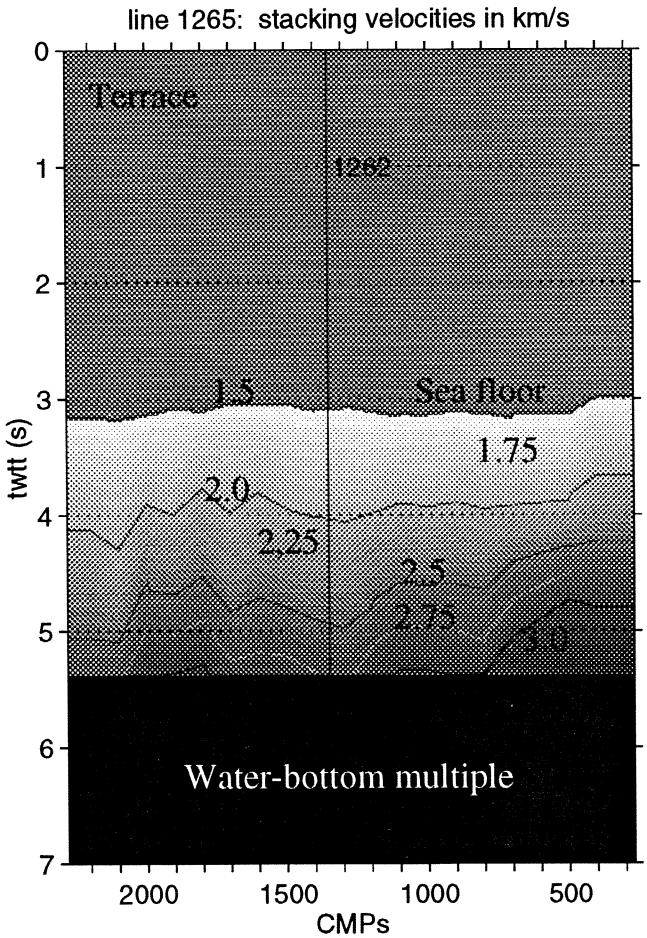

Figure 12: Two-dimensional stacking velocity distribution of line 1265 used for NMO correction; stacking velocity contours have intervals of 0.25 km/s. Velocity analyses were performed every 100th CMP. White area represents the water velocity of 1.5 km/s in shallow portions, and water-bottom multiples at depth are black.